Available online at www.sciencedirect.com
SCIENCE DIRECT®
Journal of Catalysis 229 (2005) 197–205
JOURNAL OF CATALYSIS
www.elsevier.com/locate/jcat

Promotional effect of SO_2 on the activity of Ir/SiO_2 for NO reduction with CO under oxygen-rich conditions

Masaaki Haneda [a,*], Pusparatu [b], Yoshiaki Kintaichi [a], Isao Nakamura [a], Motoi Sasaki [a], Tadahiro Fujitani [a], Hideaki Hamada [a]

[a] *Research Institute for Innovation in Sustainable Chemistry, National Institute of Advanced Industrial Science and Technology (AIST), AIST Tsukuba Central 5, 1-1-1 Higashi, Tsukuba, Ibaraki 305-8565, Japan*

[b] *Department of Materials Science and Technology, Faculty of Engineering, Gifu University, Yanagido 1-1, Gifu 501-1193, Japan*

Received 16 September 2004; revised 25 October 2004; accepted 25 October 2004

Available online 8 December 2004

Abstract

The effect of coexisting SO_2 on the activity of silica-supported noble metal catalysts for the selective reduction of NO with CO in the presence of O_2 was investigated. Pt/SiO_2, Rh/SiO_2, and Pd/SiO_2 showed little catalytic activity for NO reduction, irrespective of coexisting SO_2. Although Ir/SiO_2 showed no NO reduction activity in the absence of SO_2, the presence of SO_2 drastically promoted NO reduction. A comparison of the catalytic performance of Ir/SiO_2 and Ir/Al_2O_3 in the presence of SO_2 showed that Ir supported on SiO_2 is more active than Ir on Al_2O_3. SiO_2 was found to be a more effective support than Al_2O_3. The most outstanding feature of the reaction on the Ir/SiO_2 catalyst was that the coexistence of SO_2 and O_2 is essential for NO reduction to occur. The role of coexisting SO_2 was considered to be not only to stabilize but also to create Ir^0 sites in an oxidizing atmosphere. FT-IR measurements suggested that a *cis*-type coordinated species of NO and CO on one iridium atom ($Ir\begin{smallmatrix}NO\\CO\end{smallmatrix}$) was an intermediate for NO reduction by CO. Although the $Ir\begin{smallmatrix}NO\\CO\end{smallmatrix}$ species completely disappeared with the addition of O_2 to the reaction gas, the presence of coexisting SO_2 caused a reappearance of the $Ir\begin{smallmatrix}NO\\CO\end{smallmatrix}$ species. A reaction mechanism in which N_2 and N_2O are produced via the recombination of dissociated N atoms ($N_{(a)} + N_{(a)} \rightarrow N_2$) and the formation of dimer $(NO)_2$-type species ($2NO \rightarrow (NO)_{2(a)} \rightarrow N_2O + O_{(a)}$), respectively, is proposed.

Keywords: Selective reduction; Carbon monoxide; Nitrogen monoxide; Iridium catalyst; SO_2 promoting effect

1. Introduction

The selective reduction of NO in an oxidizing atmosphere has recently received extensive attention, since it has potential as a practical strategy for removing NO_x emitted from diesel engines, lean-burn engines, and combustors. Although NH_3 is currently used as an efficient selective reductant for flue gases from large-scale boilers, it cannot be used for small-scale or mobile NO_x sources. In this regard, a great number of studies have been made recently on the use of hydrocarbons as reductants for the selective catalytic reduction of NO (HC-SCR) [1–3]. Nevertheless, practical application of HC-SCR is not easy, because its catalytic performance is insufficient. In particular, catalyst deactivation and reaction inhibition by coexisting SO_2 and H_2O are major problems to be solved.

Hydrogen and CO were not regarded as effective reductants until recently. In 1997, Yokota et al. [4] reported the activity of Pt/mordenite for NO reduction with H_2 in the presence of O_2 around 423 K. They also found that the addition of Mo and Na widens the temperature window. Later, several researchers studied the selective reduction of NO with H_2 over Pt- and Pd-based catalysts [5–8]. As for NO reduction with CO, Ogura et al. [9] investigated the activ-

* Corresponding author. Fax: +81-298-61-4647.
E-mail address: m.haneda@aist.go.jp (M. Haneda).

0021-9517/$ – see front matter
doi:10.1016/j.jcat.2004.10.022

ity of supported iridium catalysts and found that NO can be successfully reduced to N_2 with CO over Ir/silicalite catalyst and that the catalytic activity is not influenced by coexisting SO_2. Wang et al. [10] reported that among Pt, Pd, Rh, and Ir catalysts, Ir/ZSM-5 catalyst exhibited the highest activity for NO reduction by CO in the presence of excess O_2. The selective reduction of NO with CO was also reported to take place catalytically over supported metal oxide catalysts such as Cu/Al_2O_3 [11]. Comparison of the activity of various supported metallic catalysts under the same conditions revealed, however, that the activity of Cu/Al_2O_3 is not very high, and that supported iridium catalyst is the most active for NO reduction with CO [12].

We have recently discovered that Ir/SiO_2 and Rh/SiO_2 show marked catalytic activity for NO reduction with H_2 in the presence of O_2 and SO_2 [13,14]. The most significant feature of this reaction is that the presence of SO_2, which normally poisons catalytic reactions, actually promotes NO reduction in the presence of O_2. This is quite a favorable characteristic for the treatment of diesel exhaust. However, no evidence has yet been obtained to explain this promoting effect of SO_2. In this paper, we report that CO, which is a more practical reductant than H_2, also serves as an effective reductant for NO reduction over Ir/SiO_2 catalyst in the presence of O_2 and SO_2. A mechanistic role for SO_2 is also proposed, based on in situ IR measurements.

2. Experimental

2.1. Catalyst preparation

Silica-supported noble metal (Pt, Rh, Pd, Ir) catalysts were prepared by impregnation of SiO_2 (Fuji Silysia Chemicals, Cariact G-10, 300 $m^2\,g^{-1}$) with aqueous solutions of $[Pt(NH_3)_4](NO_3)_2$ (aqueous solution, Pt content = 5.77%; N.E. Chemcat), $Rh(NO_3)_3$ (Soekawa Chemicals), $[Pd(NH_3)_4](NO_3)_2$ (N.E. Chemcat), or $H_2IrCl_6 \cdot 6H_2O$ (Soekawa Chemicals). For comparison, Ir/Al_2O_3 was also prepared by impregnation of Al_2O_3 (Mizusawa Chemicals, GB-45, 190 $m^2\,g^{-1}$) with an aqueous solution of $H_2IrCl_6 \cdot 6H_2O$. The impregnated catalyst precursors were dried at 383 K and finally calcined at 873 K for 8 h in air. The loading of noble metals was fixed at 5 wt%.

2.2. Catalytic activity measurement

Catalytic activity was evaluated with a fixed-bed continuous-flow reactor. A catalyst sample (0.04 g) was held in a quartz tube (10 mm i.d.) by quartz wool packed into both ends of the catalyst bed. Prior to each reaction, the catalyst was pretreated in situ in a flow of 10% H_2–6% H_2O/He at 873 K for 1 h, unless otherwise specified.

The standard reaction gas, containing NO (1000 ppm), CO (6000 ppm), O_2 (5%), SO_2 (20 ppm), and H_2O (6%) diluted in He as the balance gas, was fed through the catalyst bed at a rate of 90 $cm^3\,min^{-1}$ (SV = ca. 75000 h^{-1}). In some experiments, the concentration of each component gas was changed. The effluent gas was analyzed with the use of two on-line gas chromatographs equipped, respectively, with a Molecular Sieve 5A column (for the analysis of N_2 and CO) and a Porapak Q column (for the analysis of CO_2 and N_2O). The reaction temperature was reduced from 873 to 473 K in steps of 25–50 K, and the steady-state catalytic activity was measured at each temperature.

2.3. Catalyst characterization

The amount of chemisorbed CO was measured with a pulse method. The sample (0.05 g) was first reduced with H_2 at 673 K for 1 h, then cooled to room temperature in flowing He. Several pulses of CO were introduced into the sample until no more adsorption was observed.

The crystal structure was identified by XRD (Mac Science M18XHF^{22}) measurements with Cu-K_α radiation at 40 kV and 150 mA. TEM analysis was made with a Hitachi H-9000NAR at an acceleration voltage of 200 kV.

2.4. FT-IR study

Diffuse reflectance FT-IR spectra were recorded with a Nicolet Nexus 670 FT-IR spectrometer, which accumulated 64 scans at a resolution of 4 cm^{-1}. Prior to each experiment, 12 mg of a catalyst placed in a diffuse-reflectance high-temperature cell (Spectra Tech) fitted with CaF_2 windows was pretreated *in situ* by heating in flowing 10% H_2–6% H_2O/He at 873 K and then purged with He for 1 h, followed by cooling to the desired temperature. The background spectrum of the clean surface was measured for spectral correction. Surface species were observed after introduction of a reaction gas containing one or more of the gas components 1000 ppm NO, 6000 ppm CO, 5% O_2, or 20 ppm SO_2 at a flow rate of 30 $cm^3\,min^{-1}$.

2.5. Isotopic transient kinetic analysis

Isotopic transient kinetic analysis was carried out by switching the flowing gas from ^{15}NO–CO–O_2–SO_2/He to ^{14}NO–CO–O_2–SO_2/He at 523 K for a catalyst sample of 0.02 g. The effluent gas from the reactor was continuously monitored by a quadrupole mass spectrometer (ANELVA M-QA200TS) for all of the isotopic products of N_2 (at $m/e = 28,\ 29$ and 30) and N_2O (at 44, 45, and 46).

3. Results and discussion

3.1. Activity of noble metal catalysts

Table 1 summarizes the catalytic activity of the silica-supported noble metal catalysts for NO reduction with

Table 1
NO reduction with CO over supported noble metal (5 wt%) catalysts

Catalyst	O_2	SO_2	NO conversion to N_2 (N_2O) (%)							CO conversion to CO_2 (%)						
	(%)	(ppm)	423 K	473 K	573 K	623 K	673 K	723 K	773 K	423 K	473 K	573 K	623 K	673 K	723 K	773 K
Pt/SiO_2	5	0	0 (3.2)	0 (1.2)	0 (1.3)	0 (0.3)	0 (0.2)	0 (0)	0 (0)	74	100	100	100	100	100	100
	5	20	0 (0.5)	0 (1.0)	0 (0.7)	0 (0.4)	0 (0.6)	0 (0.3)	0 (0.2)	4.5	98	100	100	100	100	100
Rh/SiO_2	5	0	0 (0.3)	0 (0.7)	0 (0.2)	0 (0.2)	0 (0)	0 (0)	0 (0)	11	97	100	100	100	100	100
	5	20		0 (0.6)	0 (1.1)	0 (1.7)	0 (1.3)	0 (0.6)	0 (0.2)		2.6	12	46	95	100	100
Pd/SiO_2	5	0	0 (2.3)	0 (0.2)	0 (0.2)	0 (0)	0 (0)	0 (0)	0 (0)	95	100	100	100	100	100	100
	5	20		0 (0.7)	0 (1.2)	0 (0.7)	0 (0.5)	0 (0.2)	0 (0)		28	98	100	100	100	100
Ir/SiO_2	0	0		7.4 (2.2)	54 (3.6)	61 (2.0)	43 (1.5)	44 (0)	79 (0)		4.9	25	24	52	99	96
	5	0		0 (0)	0 (0)	0 (0)	0.7 (0.2)	0 (0)	0 (0)		2.9	77	97	100	100	100
	5	20		3.3 (0.9)	11 (2.4)	62 (6.0)	28 (3.2)	14 (1.5)	4.1 (0.8)			17	90	96	97	99
Ir/Al_2O_3	0	0		0.8 (0.9)	35 (4.6)	30 (2.8)	83 (4.8)	84 (1.2)	42 (0)		6.4	32	34	19	21	96
	5	0		0 (0)	0 (0)	1.4 (0.2)	5.7 (0.4)	12 (0.7)	7.3 (0.6)		0.9	81	98	100	100	100
	5	20		0 (0.6)	0 (0.6)	2.8 (1.1)	15 (1.9)	6.1 (1.1)	2.4 (0.3)		1.8	4.1	17	67	96	100

Conditions: NO = 1000 ppm, CO = 6000 ppm, O_2 = 0 or 5%, SO_2 = 0 or 20 ppm, H_2O = 6%, $W/F = 0.0267\ \mathrm{g\,s\,cm^{-3}}$.

6000 ppm CO in the presence of 5% O_2 either with or without 20 ppm SO_2. The reproducibility of the catalytic activity data was fairly good in this study.

Pt/SiO_2, Rh/SiO_2, and Pd/SiO_2 showed little catalytic activity for NO reduction to N_2/N_2O over the entire temperature range, irrespective of coexisting SO_2. The performance of Ir/SiO_2, on the other hand, was markedly different. Although NO reduction did not take place in the absence of SO_2, the presence of coexisting SO_2 drastically promoted NO reduction. At 623 K, for instance, the presence of 20 ppm SO_2 increased NO conversion to N_2/N_2O from 0 to 68%. In contrast to NO conversion, CO conversion was decreased by the presence of SO_2, suggesting that coexisting SO_2 improves the utilization of CO for NO reduction. In conclusion, iridium is the only active noble metal that allows NO reduction with CO in the presence of O_2 and SO_2.

3.2. Comparison of Ir/SiO_2 and Ir/Al_2O_3

Table 1 also shows the activity of Ir/Al_2O_3 catalyst. It is noteworthy that the catalytic activity of Ir/Al_2O_3 was little affected by the presence of SO_2, although a slight downward shift of the effective temperature window was observed. Thus, SiO_2 is a more effective support than Al_2O_3 for NO reduction with CO in the presence of O_2 and SO_2. The different activities of Ir/SiO_2 and Ir/Al_2O_3 may be attributable to the difference in the amount of residual chloride ions on SiO_2 and Al_2O_3. However, Ir/Al_2O_3 prepared with $Ir(NO_3)_4$ (N.E. Chemcat) as a Cl-free iridium precursor showed a catalytic performance (results not shown) similar to that prepared with $H_2IrCl_6 \cdot 6H_2O$, suggesting that the influence of residual chloride ions can be ruled out. This is probably due to the fact that chloride ions are almost completely removed by treatment with H_2–H_2O/He gas mixture before the reaction.

Table 2
Dispersion of iridium on catalysts

Catalyst	Dispersion (CO/noble metal)	Amount of CO adsorption (mol g_{cat}^{-1})
Ir/SiO_2	0.09	2.26×10^{-5}
Ir/Al_2O_3	0.05	1.34×10^{-5}

To obtain information on the physical properties of supported Ir catalysts, the amount of CO adsorption was first measured with the pulse method. As summarized in Table 2, no major difference in the amount of CO adsorption, corresponding to the number of Ir atoms exposed on the surface, was observed for Ir/SiO_2 and Ir/Al_2O_3, although the former catalyst was more active than the latter one (Table 1). This suggests that the dispersion of Ir does not significantly affect the catalytic performance.

TEM observation was also performed for Ir/SiO_2 and Ir/Al_2O_3 to examine the structure of supported Ir particles. Fig. 1 shows the TEM images of Ir/SiO_2 and Ir/Al_2O_3 treated with an H_2–H_2O/He flow at 873 K. From Fig. 1a-1, it was found that Ir particles are well dispersed with a size of 10–20 nm over the surface of the SiO_2 support. The lattice constant of Ir particles calculated from the TEM images (Fig. 1a-2) indicated the formation of the metal phase of Ir by the H_2–H_2O treatment at 873 K. This is in accordance with the results of the XRD measurements described below. On the other hand, the structure of Ir particles deposited on Al_2O_3 seems to be different from the structure of those on SiO_2 (Fig. 1b). The Ir particles on Al_2O_3 clearly consist of agglomerates of small particles with a size of 2–3 nm, and their formation is likely to be responsible for the low NO reduction activity of Ir/Al_2O_3. The rest of this paper deals mainly with Ir/SiO_2 catalyst, which showed the highest NO reduction activity.

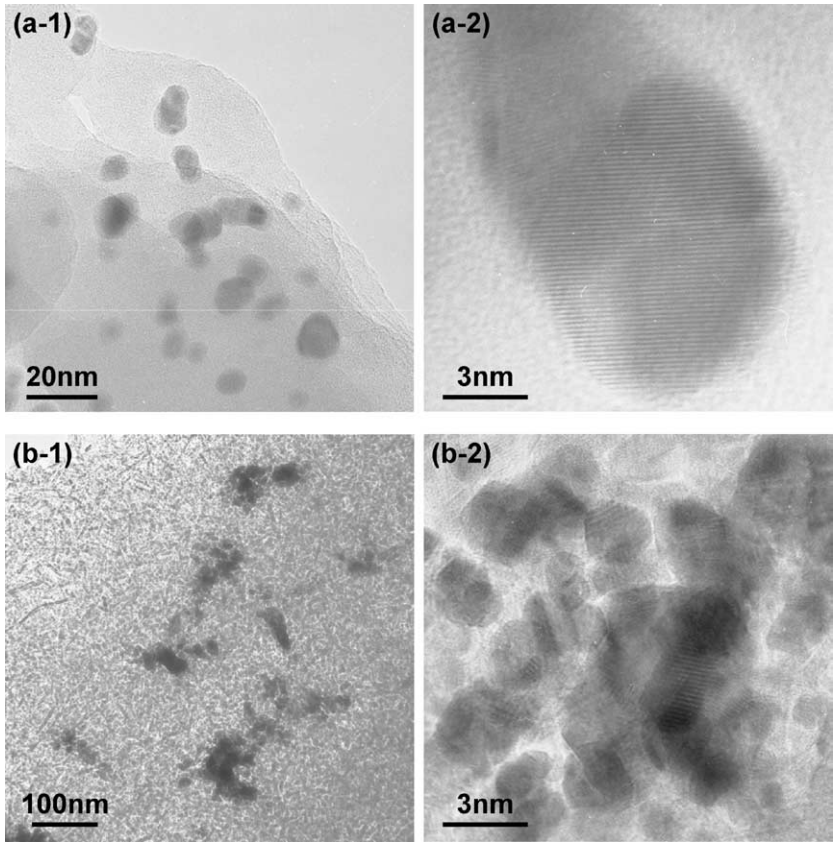

Fig. 1. TEM images of (a) 5% Ir/SiO_2 and (b) 5% Ir/Al_2O_3 treated in flowing 10% H_2–6% H_2O/He at 873 K.

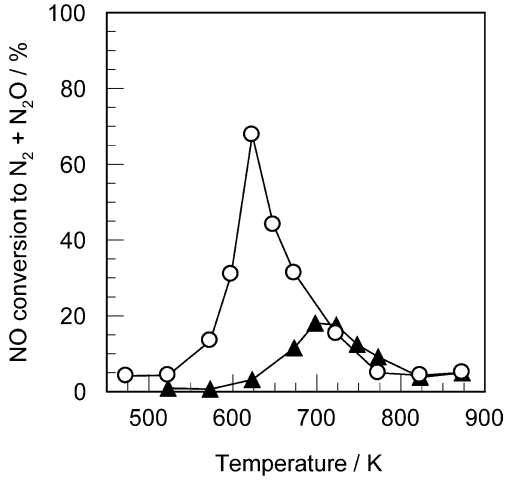

Fig. 2. Effect of pretreatment conditions on the activity of Ir/SiO_2 for NO reduction with CO in the presence of O_2 and SO_2. Conditions: NO = 1000 ppm, CO = 6000 ppm, O_2 = 5%, SO_2 = 20 ppm, H_2O = 6%, $W/F = 0.0267$ g s cm^{-3}. (▲) treated in flowing 5% O_2/He at 873 K, (○) treated in flowing 10% H_2–6% H_2O/He at 873 K.

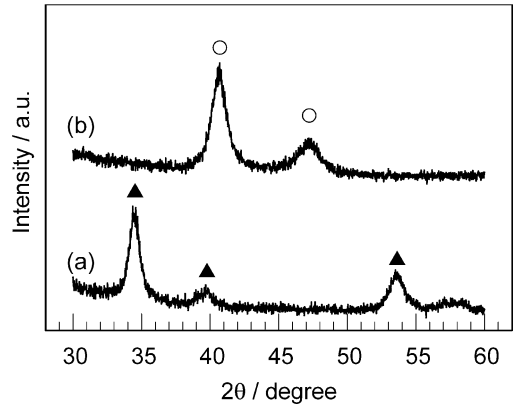

Fig. 3. XRD patterns of Ir/SiO_2 treated in flowing (a) 5% O_2/He and (b) 10% H_2–6% H_2O/He at 873 K. (▲) for IrO_2, (○) for Ir^0.

3.3. Catalytic performance of Ir/SiO_2 for NO reduction with CO

3.3.1. Effect of pretreatment condition

Fig. 2 shows the catalytic activity of Ir/SiO_2 pretreated in a flow of either 5% O_2/He or 10% H_2–6% H_2O/He at 873 K for 1 h for NO reduction with CO in the presence of O_2 and SO_2. The catalytic activity clearly depends on the pretreatment conditions. Higher activity was achieved for Ir/SiO_2 reduced with H_2–H_2O/He gas, whereas Ir/SiO_2 pretreated with O_2/He showed little activity for NO reduction. XRD patterns of Ir/SiO_2 treated with oxidizing or reducing gases are given in Fig. 3. After the treatment with oxidizing gas (Fig. 3(a)), distinct XRD peaks assignable to IrO_2 were observed, whereas diffraction lines due to Ir^0 were observed after the reduction (Fig. 3(b)). Accordingly, NO reduction with CO proceeds mainly on Ir^0 sites.

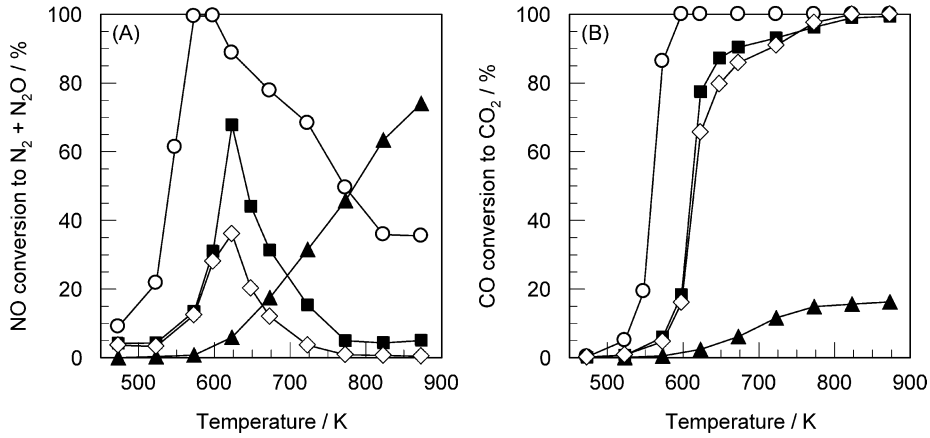

Fig. 4. Effect of O_2 concentration on (A) NO conversion to $N_2 + N_2O$ and (B) CO conversion to CO_2 for NO reduction with CO in the presence of SO_2 over Ir/SiO_2 catalyst. Conditions: NO = 1000 ppm, CO = 6000 ppm, O_2 = 0–10%, SO_2 = 20 ppm, H_2O = 6%, $W/F = 0.0267$ g s cm^{-3}. (▲) 0% O_2, (○) 1% O_2, (■) 5% O_2, (◇) 10% O_2.

3.3.2. *Effect of O_2 concentration*

From a practical viewpoint, the effect of O_2 concentration is an interesting issue. Fig. 4 presents the effect of O_2 concentration on the activity of Ir/SiO_2 for NO reduction with CO in the presence of SO_2. When O_2 was not present in the reaction gas, NO reduction did not take place at temperatures below 573 K, and the NO conversion gradually increased with increasing reaction temperature above this temperature. It is noteworthy that the NO conversion at temperatures below 773 K was significantly increased by the addition of 1% O_2, indicating that O_2 is necessary for NO reduction with CO in the presence of SO_2. However, a further increase in O_2 concentration to 10% caused a decrease in the NO conversion. Since CO conversion also decreased with increasing O_2 concentration, the negative effect of too much O_2 is not due to an increase in undesirable CO combustion. It is likely that most of the Ir^0 species that act as active catalyst components are oxidized to IrO_2 during the reaction.

3.3.3. *Effect of SO_2 concentration*

Fig. 5 shows the effect of SO_2 concentration on the activity of Ir/SiO_2 for NO reduction with CO in the presence of O_2. In the absence of SO_2, selective reduction of NO with CO did not occur. It should be noted that only a trace of SO_2 (2 ppm) is sufficient to enhance deNO_x activity. However, no change in the NO conversion was observed when SO_2 was increased to 20 ppm.

Since the promotional effect of SO_2 may be related to the change in the supported iridium species, the response of the NO conversion over Ir/SiO_2 to an intermittent feed of 20 ppm SO_2 was examined at 573 K. The results are given in Fig. 6. It is clear that the conversion of NO was rapidly increased after the introduction of SO_2. The subsequent removal of SO_2 caused a gradual reduction in the conversion of NO, and the initial low steady-state activity was resumed in 4 h. This means that the effect of coexisting SO_2 was almost completely lost after removal of SO_2 from the reaction

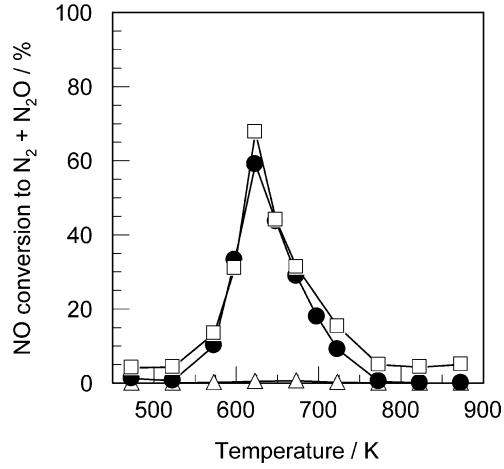

Fig. 5. Effect of SO_2 concentration on the activity of Ir/SiO_2 for NO reduction with CO in the presence of O_2. Conditions: NO = 1000 ppm, CO = 6000 ppm, O_2 = 5%, SO_2 = 0–20 ppm, H_2O = 6%, $W/F = 0.0267$ g s cm^{-3}. (△) 0 ppm SO_2, (●) 2 ppm SO_2, (□) 20 ppm SO_2.

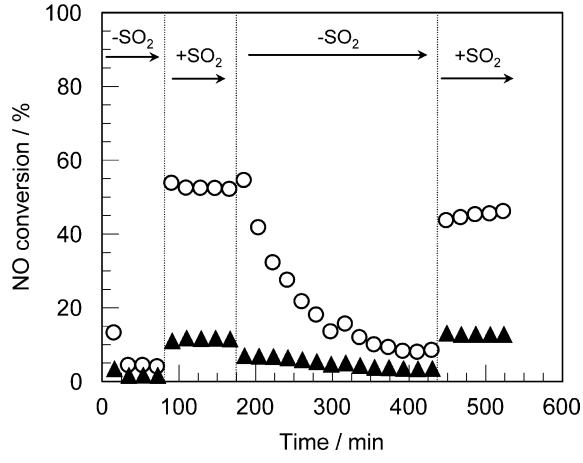

Fig. 6. Response of NO conversion to intermittent feed of 20 ppm SO_2 over Ir/SiO_2 at 573 K. Conditions: NO = 1000 ppm, CO = 6000 ppm, O_2 = 5%, SO_2 = 0 or 20 ppm, H_2O = 6%, $W/F = 0.0267$ g s cm^{-3}. (○) NO conversion to N_2, (▲) NO conversion to N_2O.

gas, suggesting that the catalytically active sites for NO reduction are created by interaction with coexisting SO_2 on the catalyst surface.

3.4. Influence of SO_2 on the structure of iridium supported on SiO_2

The fact that NO conversion gradually decreased to the initial steady state after the removal of SO_2 from the reaction gas, as illustrated in Fig. 6, suggests that SO_2 interacts with the catalyst, resulting in a change in the crystallite structure and/or surface state of iridium. To gain information on this, we measured the XRD patterns of Ir/SiO_2 after use in the reaction with or without SO_2 and the FT-IR spectra of CO species adsorbed to Ir/SiO_2 in the presence of O_2 and SO_2.

3.4.1. Study of crystallite structure by XRD

Fig. 7 shows XRD patterns for Ir/SiO_2 after use in the reaction with or without SO_2. It is apparent that only the diffraction peaks assigned to IrO_2 were observed in XRD patterns for Ir/SiO_2 samples after use in the reaction, meaning that Ir metal particles are almost completely oxidized during the reaction, irrespective of coexisting SO_2. This result suggests that coexisting SO_2 does not directly affect the crystallite structure of iridium.

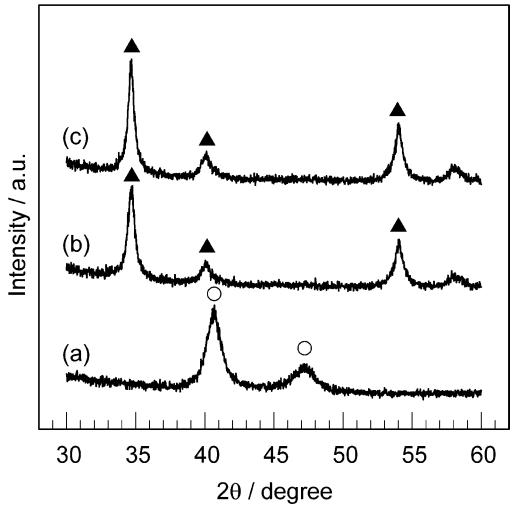

Fig. 7. XRD patterns of Ir/SiO_2 (a) before and (b) after use in the reaction without SO_2 and (c) with SO_2. (▲) for IrO_2, (○) for Ir^0.

3.4.2. Study of iridium surface by FT-IR following CO adsorption

The oxidation state of the iridium surface was investigated by FT-IR with CO as a probe molecule. This method is useful for estimating the electron density of iridium. Fig. 8 shows FT-IR spectra for CO species adsorbed on Ir/SiO_2, recorded in different compositions of flowing gas at 523 K. When 0.6% CO/He was exposed to Ir/SiO_2 (Fig. 8A(a)), a strong IR band at 2079 cm^{-1} assignable to CO linearly bonded to Ir^0 sites [15–17] was observed. The exposure of CO in the presence of O_2 to Ir/SiO_2 gave rise to an IR band at 2107 cm^{-1} (Fig. 8A(b)). A shift of the IR band to a higher wavenumber is often observed when CO is adsorbed on an oxidized metal surface [18–20]. Therefore, the IR band at 2107 cm^{-1} can be ascribed to linearly bonded CO adsorbed on $Ir^{\delta+}$ sites [20,21], indicating that the surface of iridium is almost completely oxidized in the presence of O_2.

On the other hand, when CO was exposed to Ir/SiO_2 in the presence of O_2 and SO_2 (Fig. 8A(c)), two distinct IR bands assignable to Ir^0–CO and $Ir^{\delta+}$–CO were observed at

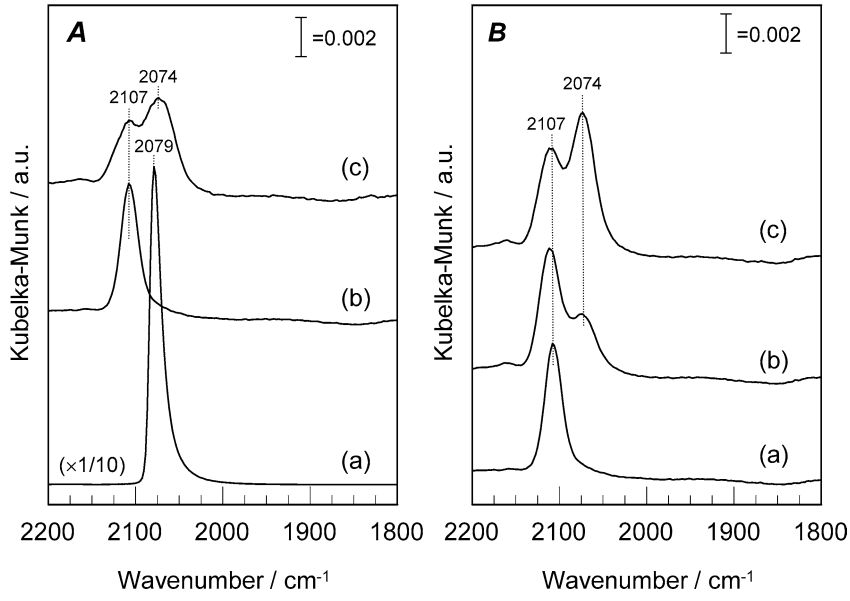

Fig. 8. (A) FT-IR spectra of CO adsorbed on Ir/SiO_2 after the exposure of (a) 0.6% CO/He, (b) 0.6% CO–5% O_2/He and (c) 0.6% CO–5% O_2–20 ppm SO_2/He at 523 K for 30 min. (B) FT-IR spectra of CO adsorbed on Ir/SiO_2 after introducing 20 ppm SO_2 into the 0.6% CO–5% O_2/He flowing for (a) 0, (b) 15 and (c) 30 min.

2074 and 2107 cm^{-1}, respectively. This clearly indicates that coexisting SO_2 participates in the stabilization of Ir^0 sites on which NO reduction with CO proceeds. It should be noted that the introduction of SO_2 into CO–O_2/He flowing gas caused the appearance of an IR band at 2074 cm^{-1} due to Ir^0–CO, and its band intensity increased with time on stream (Fig. 8B). Accordingly, the role of coexisting SO_2 is not only to stabilize but also to create Ir^0 sites in an oxidizing atmosphere. More detailed studies on how SO_2 promotes the reduction of iridium surface are now in progress that are using a surface science approach and a single-crystal model catalyst. In brief, the disproportionate occurrence of SO_2 takes place on the Ir(111) surface: $3SO_{2(a)} \rightarrow 2SO_{3(a)} + S_{(a)}$. SO_3 is thermally desorbed, and the atomic sulfur reacts with surface oxygen on iridium: $S_{(a)} + 2O_{(a)} \rightarrow 2SO_{2(g)}$. The iridium surface, thus, reverts to its initial metallic state. More detailed results will be reported elsewhere [22].

3.5. Observation of surface species formed in NO reduction over Ir/SiO_2

To investigate the effect of SO_2 on the behavior of surface-adsorbed species formed during NO reduction with CO, in situ IR spectra were measured at 523 K, at which temperature the catalytic activity is low enough for surface intermediates to be observed. Fig. 9 illustrates in situ IR spectra of adsorbed species on Ir/SiO_2 in contact with a series of gas flows containing some of the selected gas components. In flowing NO/He (spectrum (a)), an IR band assignable to NO linearly adsorbed on iridium (Ir–$NO^{\delta+}$) [15] was detected at 1842 cm^{-1}. Exposure to CO also gave an IR band at 2080 cm^{-1} due to CO species adsorbed on iridium (Ir–CO) [15–17] (spectrum (b)). When a mixture of NO + CO was introduced (spectrum (c)), the IR bands due to NO and CO at 1842 and 2080 cm^{-1} shifted to 1798 and 2060 cm^{-1}, respectively. The shift of the NO band to a lower wavenumber due to surface interaction with CO was reported for Rh/Al_2O_3 [23] and Ir/Al_2O_3 [24]. This shift is explained by the perturbing effect of adsorbed CO, suggesting the formation of *cis*-type coordinated species of NO and CO with one metal atom ($M\begin{smallmatrix}NO\\CO\end{smallmatrix}$) [23,24]. Accordingly, the IR bands at 1798 and 2060 cm^{-1} observed here can be attributed to the formation of $Ir\begin{smallmatrix}NO\\CO\end{smallmatrix}$ species.

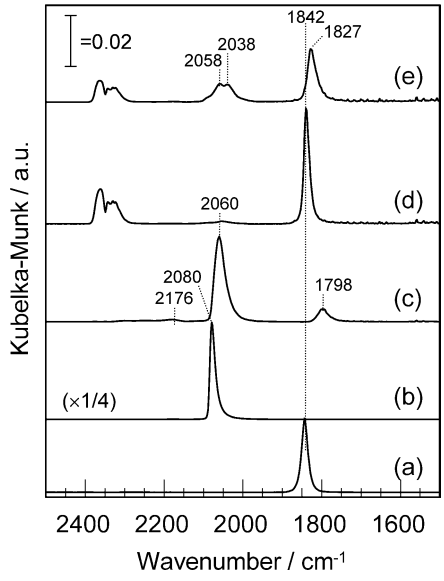

Fig. 9. In situ IR spectra of adsorbed species formed on Ir/SiO_2 in a flow of (a) NO, (b) CO, (c) NO + CO, (d) NO + CO + O_2, and (e) NO + CO + O_2 + SO_2 at 523 K for 30 min. Conditions: NO = 1000 ppm, CO = 6000 ppm, O_2 = 5%, SO_2 = 20 ppm.

It has been reported that the $M\begin{smallmatrix}NO\\CO\end{smallmatrix}$ species can be decomposed to give CO_2 and nitride (M–N), which can react with NO and CO to produce N_2O and NCO, respectively [24]. In fact, as can be seen in Fig. 9 (spectrum (c)), a very weak IR band due to the NCO species adsorbed on iridium (Ir–NCO) [25] was detected at 2176 cm^{-1} for Ir/SiO_2. It is noteworthy that Ir/SiO_2 showed high activity for NO reduction by CO in the absence of O_2 and SO_2 (Table 1). This suggests that the $Ir\begin{smallmatrix}NO\\CO\end{smallmatrix}$ species is a possible intermediate for NO reduction by CO. The fact that the bands at 1804 and 2042 cm^{-1} disappeared completely with the addition of O_2 to the NO + CO mixture (spectrum (d)) also supports this idea, since NO reduction by CO did not take place over Ir/SiO_2 in the presence of O_2 (Table 1).

Interestingly, the addition of SO_2 to the reaction gas again caused a shift of the 1842 cm^{-1} band to lower wavenumbers and the appearance of IR bands at 2038 and 2058 cm^{-1} (spectrum (e)). These band features are very similar to those obtained in the flow of NO + CO (spectrum (c)). To be exact, the $Ir\begin{smallmatrix}NO\\CO\end{smallmatrix}$ surface species can be produced during NO reduction by CO in the presence of O_2 and SO_2. However, the band features in spectrum (e) are slightly different from those in spectrum (c). The 2038 cm^{-1} band was observed in the presence of O_2 and SO_2, suggesting that new adsorption sites for CO are created by the interaction of O_2 and SO_2 over iridium, as described above (Section 3.4). Such interaction may affect the electron donation from Ir to NO by adsorption of SO_2 and/or SO_3, resulting in a shift of the N–O vibrational frequency to a slightly higher value (1842 cm^{-1}) than that detected for NO + CO (1798 cm^{-1}; spectrum (c)).

From the above-mentioned results, we can conclude that coexisting SO_2 appears to play an important role in the formation of the $Ir\begin{smallmatrix}NO\\CO\end{smallmatrix}$ surface species, resulting in significant activity enhancement (Table 1). This is probably due to the fact that Ir^0 sites can be created by coexisting SO_2, as described in the previous section. Specifically, the formation of the $Ir\begin{smallmatrix}NO\\CO\end{smallmatrix}$ surface species takes place only on Ir^0 sites, after which various reactions, leading to the formation of N_2, consecutively proceed. On the other hand, CO oxidation is likely to occur predominantly on $Ir^{\delta+}$ sites, because $Ir^{\delta+}$ sites do not have the ability to form $Ir\begin{smallmatrix}NO\\CO\end{smallmatrix}$ surface species.

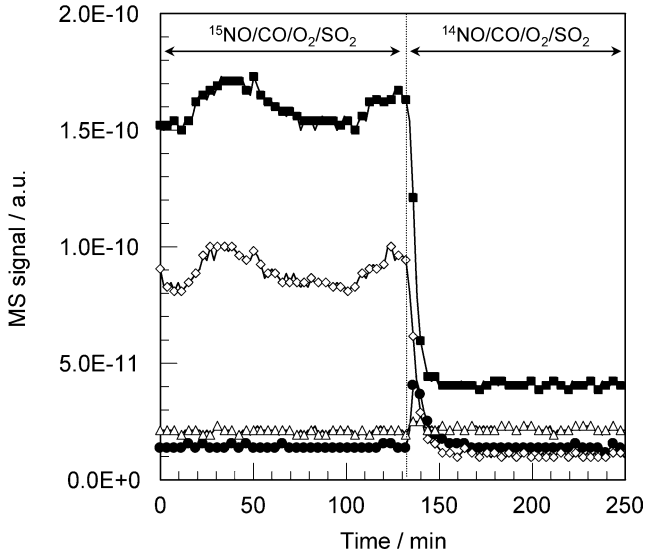

Fig. 10. Product responses when ^{15}NO is replaced with an equal quantity of ^{14}NO in a NO–CO–O_2–SO_2/He mixture for Ir/SiO_2 at 523 K. Conditions: NO = 1000 ppm, CO = 6000 ppm, O_2 = 5%, SO_2 = 20 ppm. $^{14}N^{15}N$ (●), $^{15}N_2$ (■), $^{14}N^{15}NO$ (△), $^{15}N_2O$ (◇).

3.6. Proposed reaction pathway

From the FT-IR measurements, *cis*-type coordinated species of NO and CO with one iridium atom ($Ir\begin{smallmatrix}NO\\CO\end{smallmatrix}$) are considered to be a possible intermediate for the selective reduction of NO with CO in the presence of O_2 and SO_2 over Ir/SiO_2. The participation of the same twin species of NO and CO as reaction intermediates has been reported for the NO + CO reaction over Rh/Al_2O_3 [23] and Ir/Al_2O_3 catalysts [24]. According to these reports, NO reduction with CO proceeds as follows:

$$Ir\begin{smallmatrix}NO\\CO\end{smallmatrix} \rightarrow Ir\text{–}N + CO_2, \quad (1)$$

$$Ir\text{–}N + Ir\text{–}N \rightarrow 2Ir + N_2, \quad (2)$$

$$Ir\text{–}N + NO \rightarrow Ir\text{–}NNO \rightarrow Ir + N_2O, \quad (3)$$

$$Ir\text{–}N + CO \rightarrow Ir\text{–}NCO. \quad (4)$$

In the present study, the reaction can be expected to proceed via a similar pathway. To gain detailed information on the reaction pathway, an isotopic transient kinetic analysis was made. Fig. 10 shows the isotopic product responses following the ^{15}NO–CO–O_2–SO_2/He → ^{14}NO–CO–O_2–SO_2/He switch over Ir/SiO_2 catalysts at 523 K, where the responses of unlabeled N_2 and N_2O are not given because of the overlapping mass numbers of CO and CO_2, respectively. The labeled $^{15}N_2$ and $^{15}N_2O$ were stably produced during the ^{15}NO–CO–O_2–SO_2 reaction. Interestingly, the mixed-labeled N_2 ($^{14}N^{15}N$) profile peaked very soon after the switch. This suggests that the formation of N_2 follows Eq. (2), that is, the recombination of dissociated N atoms.

On the other hand, no evolution of $^{14}N^{15}NO$ was observed. If the formation of N_2O followed Eq. (3), $^{14}N^{15}NO$ would be formed after the switch. We can state, therefore, that there is another route of formation of N_2O. Concerning N_2O formation during the NO reduction, Burch et al. [26,27] and Roberts [28] proposed a route via formation of dimer $(NO)_2$-type species as a favorable mechanism of N_2O formation over Pt catalysts:

$$2NO \rightarrow (NO)_{2(a)} \rightarrow N_2O + O_{(a)}. \quad (5)$$

If the formation of dimer $(NO)_2$ species and subsequent decomposition to N_2O were very rapid, no evolution of $^{14}N^{15}NO$ would be observed. Accordingly, the formation of N_2O in the NO reduction with CO over Ir/SiO_2 would follow Eq. (5).

4. Conclusions

Ir/SiO_2 shows very good activity with respect to NO reduction with CO in the presence of O_2 and SO_2, giving it a potential for application to NO_x removal from diesel and lean-burn engine exhaust gas. Coexisting SO_2 appears to play an important role in creating and stabilizing the Ir^0 sites on which NO reduction proceeds, resulting in the formation of the $Ir\begin{smallmatrix}NO\\CO\end{smallmatrix}$ species as a possible reaction intermediate. The formation of N_2 and N_2O from NO takes place via the recombination of dissociated N atoms ($N_{(a)} + N_{(a)} \rightarrow N_2$) and the formation of dimer $(NO)_2$-type species ($2NO \rightarrow (NO)_{2(a)} \rightarrow N_2O + O_{(a)}$), respectively.

Acknowledgment

The authors are grateful to Mr. Makoto Oishi for taking the TEM microphotographs of the samples.

References

[1] W. Held, A. Koenig, T. Richter, L. Puppe, SAE Paper 900496, 1999.
[2] H. Hamada, Catal. Today 22 (1994) 21.
[3] R. Burch, J.P. Breen, F.C. Meunier, Appl. Catal. B 39 (2002) 283.
[4] K. Yokota, M. Fukui, T. Tanaka, Appl. Surf. Sci. 121/122 (1997) 273.
[5] R. Burch, A.A. Shestov, J.A. Sullivan, J. Catal. 188 (1999) 69.
[6] A. Ueda, T. Nakao, M. Azuma, T. Kobayashi, Catal. Today 45 (1998) 135.
[7] N. Macleod, R.M. Lambert, Chem. Commun. (2003) 1300.
[8] M. Machida, S. Ikeda, D. Kurogi, T. Kijima, Appl. Catal. V 35 (2001) 107.
[9] M. Ogura, A. Kawamura, M. Matsukata, E. Kikuchi, Chem. Lett. 29 (2000) 146.
[10] A. Wang, L. Ma, Y. Cong, T. Zhang, D. Liang, Appl. Catal. B 40 (2003) 319.
[11] T. Yamamoto, T. Tanaka, R. Kuma, S. Suzuki, F. Amano, Y. Shimooka, Y. Kohno, T. Funabiki, S. Yoshida, Phys. Chem. Chem. Phys. 4 (2002) 2449.
[12] M. Shimokawabe, N. Umeda, Chem. Lett. 33 (2004) 534.
[13] T. Yoshinari, K. Sato, M. Haneda, Y. Kintaichi, H. Hamada, Catal. Commun. 2 (2001) 155.
[14] T. Yoshinari, K. Sato, M. Haneda, Y. Kintaichi, H. Hamada, Appl. Catal. B 41 (2003) 157.

[15] F. Solymosi, J. Raskó, J. Catal. 62 (1980) 253.
[16] F. Solymosi, É. Novák, A. Molnár, J. Phys. Chem. 94 (1990) 7250.
[17] A. Bourane, M. Nawdali, D. Bianchi, J. Phys. Chem. B 106 (2002) 2665.
[18] M.A. Vannice, S.-Y. Wang, S.H. Moon, J. Catal. 71 (1981) 152.
[19] W. Daniell, H. Landes, N.E. Fouad, H. Knözinger, J. Mol. Catal. A 178 (2002) 211.
[20] D. Tessier, A. Rakai, F. Bozon-Verduraz, J. Chem. Soc., Faraday Trans. 88 (1992) 741.
[21] E. Iojoiu, P. Gélin, H. Praliaud, M. Primet, Appl. Catal. A 263 (2004) 39.
[22] T. Fujitani, I. Nakamura, M. Haneda, H. Hamada, in preparation.
[23] H. Arai, H. Tominaga, J. Catal. 43 (1976) 131.
[24] F. Solymosi, J. Raskó, J. Catal. 63 (1980) 217.
[25] J. Raskó, F. Solymosi, J. Catal. 71 (1981) 219.
[26] R. Burch, A.A. Shestov, J.A. Sullivan, J. Catal. 188 (1999) 69.
[27] R. Burch, Top. Catal. 24 (2003) 97.
[28] M.W. Roberts, Catal. Lett. 93 (2004) 29.